

Investigating the effect of material stiffness contrast on the dynamic stability of upstream tailings dams (Case study: Esfordi tailings dam)

R. Salamat Mamakani¹, A. Azhari^{1*}, L. Faramarzi¹, H. Share Isfahani²

1- Dept. of Mining Engineering, Isfahan University of Technology, Isfahan, Iran

2- Dept. of Civil Engineering, Isfahan University of Technology, Isfahan, Iran

* Corresponding Author: aazhari@iut.ac.ir

(Received: March 2022, Accepted: September 2022)

Keywords

Mine Tailings dams
Numerical Methods
Liquefaction
Dynamic Analysis
Soil Mechanical Properties

Abstract

The effect of mechanical properties of upstream tailings dams is investigated under seismic loads. For this, the finite-difference numerical method under the Finn-Byrne nonlinear elastoplastic constitutive model was implemented. Variations of elastic modulus and Poisson's ratio in the typical range of tailings dam material were investigated in the phenomenon of liquefaction, horizontal displacement, and subsidence. The results showed that with increasing the elastic modulus of the dam body from 10 to 50 MPa, the maximum horizontal displacement, subsidence, and liquefaction

coefficient in the dam body have increased 2.3, 3.5, and 2 times, respectively. Moreover, by increasing the Poisson's ratio from 0.25 to 0.4, the maximum horizontal displacement, subsidence, and liquefaction coefficient in the dam body have raised 2.4, 2.3, and 1.75, respectively. The Poisson's ratio of tailings had a significant effect on the liquefaction of the dam body. In which, increasing the Poisson's ratio from 0.25 to 0.4, the maximum liquefaction coefficients were increased 1.75 times. Ultimately, it is concluded that despite the displacement which is not affected by the variation of tailings dam elastic modulus, the liquefaction coefficient is doubled by its variation, which may cause a serious threat to the stability of the dam.

1. INTRODUCTION

Site effects are defined as the effect and mechanism of local geological conditions, including topography and mechanical properties of constituent layers, on seismic wave propagation [1]. The effect of structural geometry and geomechanical characteristics on the dynamic stability of structures has been studied by researchers [2-4].

The stability of tailings dams has always been one of the challenges that have attracted the attention of researchers in this field. Tailing dams can fail due to static and dynamic loads. The static analysis of these structures is examined early in its construction and usually static loads do not undergo significant changes during the life of tailings dams. However, dynamic loads are constantly evolving and many factors can change

the way waves propagate and thus the impact of these dynamic loads on tailings dams.

Geomechanical properties of tailings dam materials can be changed by increasing their height according to the materials available to build the dam body. Also, the tailings behind the dam change the life of these structures, the most important of which is the change of their elastic modulus and Poisson's ratio. The difference in stiffness and Poisson's ratio of the materials through which seismic waves travel is constantly changing may greatly affect the occurrence of liquefaction. This phenomenon is one of the main issues regarding the dynamic stability of upstream dams. Limited studies are performed on this issue in tailings dams compared to other geotechnical structures such as landfills and slopes. The following presents several studies conducted on these types of structures.

Using numerical and laboratory methods, Havenith et al. (2002) investigated the effect of

local factors on the dynamic stability of slopes in Kyrgyzstan. They examined the natural slopes under seismic load with different frequencies and different inclinations and concluded that low frequencies have the greatest effect on the slope crests. They also concluded that the presence of a weak surface layer with different thicknesses at low wave velocities could control the slope failure [5]. Wang and Hao (2002) studied the effect of local conditions on the seismic response of slopes using numerical analyses. They applied SH, P, and SV waves to the soil layers and the effect of local factors on the propagation of waves, change in acceleration at different locations of the structure, and the intensity of wave amplification using a numerical method. They also performed a parametric study on the shear modulus, damping ratio, rock mass density, and groundwater level within the soil layer. They ultimately found that the wave amplification is highly dependent on the wave frequency as well as the site characteristics. They stated that if the multiplying factor of shear modulus, damping ratio, and rock mass density is equal, changes in shear modulus and rock mass density can have a greater effect on ground motion than the damping ratio [6].

Using the finite element numerical method in two and three dimensions, Havenith et al. (2003) investigated the effect of local characteristics such as slope angle and the presence of weak layers on the Ananevo rocky slope. For this, they applied a seismic load to the slope and studied the amplification of the wave and the slope displacements under the different local conditions. They concluded that the presence of weak layers that cover the rock slope is very important and also the presence of faults in the area, which is one of the local factors, can have a great impact on the seismic response. From the results of the field studies and experiments, as well as two-dimensional and three-dimensional analyses of the slope, they stated that the influence of local factors on the intensification of waves and earthquakes is very obvious and important [7]. Psarropoulos et al. (2007) used numerical methods to investigate the local effects on the dynamic stability of landfills. Different seismic loads, including real earthquakes and Ricker waves, and various local parameters. The researchers concluded that local parameters have a great influence on the stability of landfills; however, these parameters alone should not be the basis of the design of these structures, but also the characteristics of the landfill should be included. They also conducted sensitivity analyses on different parameters of the seismic waves and studied the wave intensification in different locations of the slope crest. They concluded that

the local parameters have a significant effect on the dynamic load and thus the stability of the landfill [8].

In another study, Bourdeau and Havenith (2008) investigated the effect of local parameters on the stability of natural slopes in Kyrgyzstan under the 1992 Suusamyр earthquake using a two-dimensional finite difference numerical method. Their analysis showed that the effect of topographic changes is less than the changes in the geological characteristics of the layers, especially the stiffness contrast between the bedrock and the surface layers of the slope. They stated that the slope failures could not have occurred solely due to the intensification of the wave, but they believe that the increase in pore water pressure along with the wave amplification on the slope is the main cause of the failures during the Suusamyр earthquake in 1992 [9]. Mitani et al. (2012) used the finite element method and ABAQUS software and evaluated the wave amplification resulting from different geological and topographic parameters of the site and its effect on a slope containing layers of tuff and shale. In the first stage, a slope consisting of different layers of tuff and shale was analyzed by changing the height, slope angle, and seismic parameters. They also monitored the intensification of the wave in two directions, east-west, and north-south. They found that as the height increased at the mid-height slope, the amplification factor decreased. Whereas it increases relatively for the higher slope angles. No significant trend for the amplification factor was observed for different geological conditions at different slope angles [10].

Moore et al. (2012) evaluated the stability of a jointed rock slope located in an earthquake-prone area in Switzerland using a two-dimensional discrete element code. They performed sensitivity analyses on the joint set stiffness and monitored the seismic response for different locations of the slope. They concluded that at some frequencies, the amplification factor increases up to 8 times, which was significant for the dynamic stability of the desired slope; whereas this parameter is not considered in most slope designs [11]. Gouveia (2012) investigated the effect of the stiffness contrast of parallel and inclined soil layers on their dynamic stability. The finite element codes SAP2000 and FLUSH were used and the amplification factor and the motion of the layers in different states were monitored. They concluded that when the soil layers are inclined, the amplification factor is higher, and also by decreasing the wave frequency, the slope motion intensifies [12]. Azhari and Ozbay (2017) used a finite element approach to investigate the effect of

geometry and stiffness contrast of materials under seismic waves due to the dynamic loading of open-pit mines, natural slopes, and tailings dams. They carried out the study by forming a database of 177 open-pit mines, of which 75 mines were located in active seismic areas. It was concluded that the narrow edges and topsoil above the natural slopes and the geometry of the shaped hills, and the unconsolidated top layer of tailings dams may intensify the maximum horizontal velocity of the earth 8 times greater than the open pit slopes. The researchers also found that varying the stiffness contrasts of 1.2 and 1.5, is amplified 1.2 and 1.8 times compared to non-layers slopes, respectively [13]. Using a finite element code, Solans et al. (2019) investigated the effect of different soil layers on the acceleration amplification in a valley-shaped slope under a harmonic wave load. They concluded that the maximum acceleration amplification occurs at the boundary between two soil layers with different stiffnesses. They also stated that the amplification factor increases for non-uniform soils in the canopy of shaped canyon and for the case where the input period is less than 0.33 seconds [14]. Azhari et al. (2021) conducted a study on the effect of geometry and stiffness contrast of landfill material using a numerical method on wave intensification and their dynamic stability. They monitored and recorded the amplification factor for six common landfill geometries at different points. The researchers found that for low stiffness contrasts, stepped base and hill-shaped landfill types had the lowest (1.74) and highest (3.53) amplification factors, respectively. However, for high stiffness contrasts, the valley-shaped landfill recorded the lowest amplification due to the damping effect and tailings thickness [15].

Tailings dams are subjected to a consolidation process during the life of the mine, thus change in the material properties such as elastic modulus and Poisson's ratio. According to previous studies, this may cause instabilities during seismic loads if not considered in their design. However, the effect of site characteristics, especially stiffness contrast on the seismic response of these structures has not been extensively examined. In this study, the effect of mechanical parameters that may change during the life of the tailings dam under sinusoidal seismic waves was evaluated using a nonlinear elastoplastic constitutive model and finite difference numerical approach. The data of the Esfordi tailings dam located in the seismically active area in central Iran were used as the case study.

2. THE STUDY AREA AND SITE CHARACTERISTICS

Esfordi tailings dam is located in Bafgh city, Yazd province as one of the earthquake-prone regions subjected to several large earthquakes. This tailings dam is constructed using the upstream method which is known to be susceptible to seismic instability [16]. Figure 1 depicts a schematic view of the dam geometry.

As shown the dam consists of three parts, the foundation, the body, and the tailings. The height of the dam is 8 meters and the slope angle of the dam body is 45 degrees. The crest height of the dam body is considered one meter higher than the tailings to prevent tailings from overflowing. The physical and geomechanical properties of the components of this tailings dam are presented in Table 1.

According to table 1, it can be seen that the elastic modulus of the foundation is significantly different between the tailings and dam body. This high stiffness contrast considerably affects its seismic response.

3. EMPLOYED CONSTITUTIVE MODELS

To model the Esfordi tailings dam, FLAC2D code was used, implementing the Finn-Byrne constitutive model. The Finn-Byrne constitutive model is able to simulate the strain increase due to each loading cycle during the dynamic load which is defined as below [17, 18].

$$(\Delta\varepsilon_v)_{\frac{1}{2}\text{cycle}} = \gamma_c C_1 e^{\left(-C_1 \frac{\varepsilon_{vd}}{\gamma_c}\right)} \quad (1)$$

where $(\Delta\varepsilon_v)_{\frac{1}{2}\text{cycle}}$ indicates the change in the volumetric strain in each of the half-cycles (loading-unloading), ε_{vd} is the volumetric strain stored up to the previous cycle (%), γ_c is the shear strain amplitude for each cycle (%), and C_1 and C_2 are constants that C_1 is obtained from the following relation [18, 19].

$$C_1 = 7600(D_r)^{-2.5} \quad (2)$$

where D_r is the relative density of the sample. The obtained C_1 values for the dam body and tailings are 0.65 and 1.54, respectively. The constant C_1 can also be obtained by holding the normalized standard penetration value $(N_1)_{60}$ using Equation 4 [20].

$$C_1 = 8.7((N_1)_{60})^{-1.25} \quad (3)$$

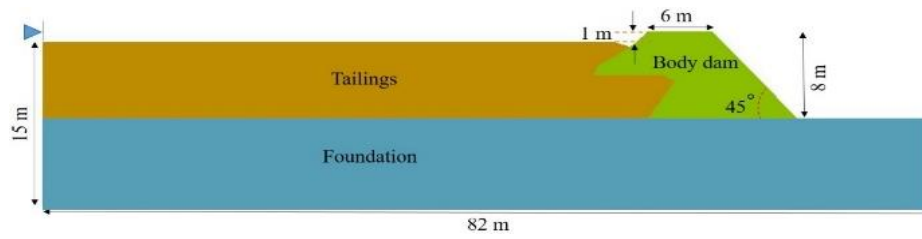


Fig. 1. Schematic of Esfordi tailings dam [16].

Table 1. Physical and geomechanical parameters of Esfordi tailings dam [16]

Material type	γ_{unsat} ($\frac{\text{kg}}{\text{m}^3}$)	C (kPa)	ϕ ($^\circ$)	E (MPa)	ν	k ($\frac{\text{m}}{\text{s}}$)	e (%)	$(N_1)_{60}$
Body dam	2900	17.72	25.36	20	0.25	10^{-8}	4	8
Tailings	2320	6.16	26.3	5	0.25	10^{-7}	10	4
Foundation	2900	1000	40	5000	0.2	10^{-9}	1	-

The relative density and the normalized value of the standard penetration test have the following relationship with each other, where one can also derive the other [19].

$$D_r = 15((N_1)_{60})^{0.5} \quad (4)$$

Where based on the $(N_1)_{60}$ values presented in Table 2, the relative densities of the dam body and tailings were derived to be 42/4 and 30, respectively.

The second constant C_2 , which is a ratio of the first constant C_1 is calculated from the following equation [18, 19].

$$C_2 = \frac{0.4}{C_1} \quad (5)$$

The C_2 constant of the dam body and tailings were obtained at 0.62 and 0.26, respectively.

After defining the constitutive model for the dam body and tailings, and assigning the Mohr-Columb constitutive model to the dam foundation model, boundary conditions have been considered for both static and dynamic analyses. In the static models, fixed displacements at the boundaries, pore pressure, and saturation in the dam body and tailings are considered. For the dynamic analyses, the boundaries are defined as free-field and quiet boundaries, as shown in Figure 2, since the seismic load is applied to the model as shear stress.

Since the purpose of this study is to investigate the effect of local parameters on the dynamic stability of the tailings dam, the effect of wave type and duration is not considered. As a result, a typical sinusoidal wave with a PGA of 0.5g, frequency of 5 Hz, and one-second duration is applied to the bottom of the model in terms of shear stress in two vertical and horizontal

components. Figure 3 shows the sinusoidal wave applied at the bottom of the model.

Equation 6 is used to convert the acceleration against time to the applied shear stress.

$$C_s = \left(\frac{E}{2\rho(1+\nu)} \right)^{0.5} = \left(\frac{G}{\rho} \right)^{0.5} \quad (6)$$

where C_s is the shear velocity (m/s). The shear velocity would be 52.5 m/s in the dam body.

Mesh dimension is one of the important parameters in numerical modeling that if they exceed a specific size, the wave will not propagate properly through the model; also, for very small mesh sizes, the solution time of the model would greatly increase and in both cases, the probability of error occurrence will increase. For this, the mesh dimension should not exceed one-tenth of the wavelength using the equation below [21].

$$\Delta l_{\text{max}} = \frac{C_s}{10f_{\text{max}}} \quad (7)$$

where f_{max} is the maximum frequency (Hz) at which the wave has power. Examining the earthquakes in the Bafgh region their maximum wave power amplitude occurs mostly at the frequency of 6 Hz [22]. As a result, in this study, a frequency of 6 Hz is assumed for the harmonic wave. According to equations (6) and (7), the maximum dimensions of the mesh should be approximately one meter.

Another important parameter in geotechnical numerical modeling is the applied damping coefficient. Damping of geological materials is usually in the range of 2 to 5% of critical damping. In this study, Rayleigh damping of 5% was used for the simulations.

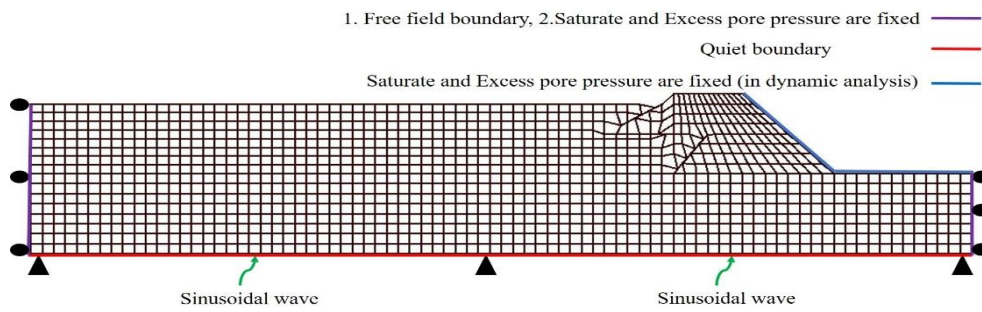


Fig. 1. Boundary conditions of the static and dynamic mods.

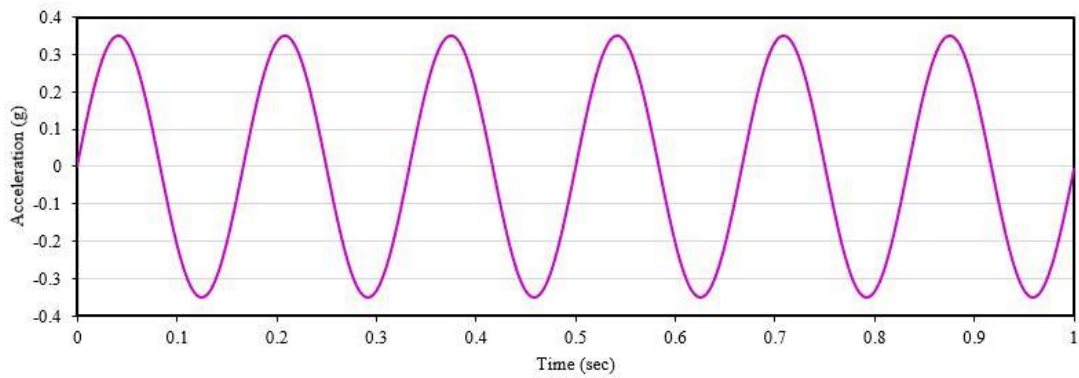


Fig. 3. Sinusoidal wave applied at the bottom of the model (PGA:0.5g, Frequency: 5 Hz, Duration 1sec).

4. STATIC AND DYNAMIC STABILITY ANALYSES OF THE DAM'S SLOPE

After implementing the static and dynamic considerations for the simulations, the effect of stiffness contrast of the dam materials on its seismic response is examined by changing the elastic modulus and Poisson's ratio of different parts of the dam. First, the changes of the elastic modulus are examined where the range of changes of this variable can be seen in Table 2.

Table 1. Variation of stiffness contrast

Parameter	E(MPa)	SC	K(MPa)	G(MPa)
Body Dam	10-50	500-100	6.67-33.33	4-30
Tailings	2-10	2500-500	1.33-6.67	0.8-4

Displacement and liquefaction are the two key parameters in the dynamic stability analysis of tailings dams which could be significantly affected by the stiffness contrast of the dam material. Figure 4 illustrates the displacement variation caused by the change in the stiffness contrast between the foundation and dam body material. It is observed that with increasing the stiffness contrast between the foundation and the dam body, the maximum horizontal displacement and the absolute value of the maximum vertical displacement in the dam body have decreased. This trend can be due to the weakening of the dam body material with increasing stiffness contrast

thus more wave attenuation while passing through the material occurs. It is noteworthy that with the increasing stiffness difference between the foundation and the body of the dam, at the boundary between these two layers, with the passage of a wave through the hard material and its sudden entry into the weak material, the displacement increases momentarily. This increase fades while the wave travels through the weak material due to its high damping ratio. Figure 5 illustrates the horizontal and vertical displacement contours of the Esfordi tailings dam.

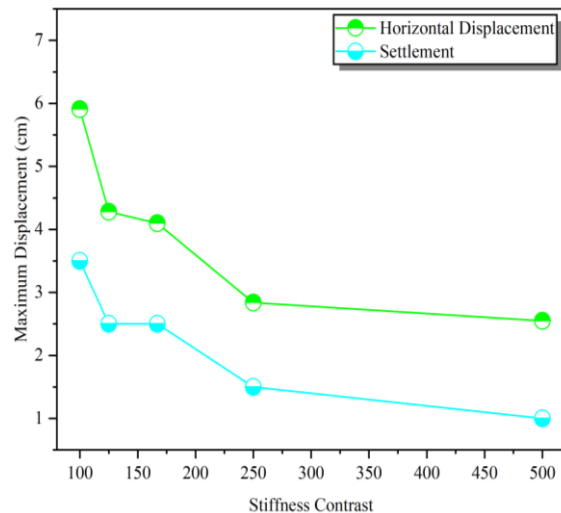


Fig. 4. Displacements occur from variations in the stiffness contrast between the foundation and dam body material.

The displacement contours in Figure 5 show that in general, displacement and subsidence have occurred in the entire dam body and tailings; However, its values of the slope surface and the crest are much higher than in other parts. Where

the maximum horizontal displacement occurred in the mid-height of the dam, and the largest subsidence is observed in the middle of the dam crest.

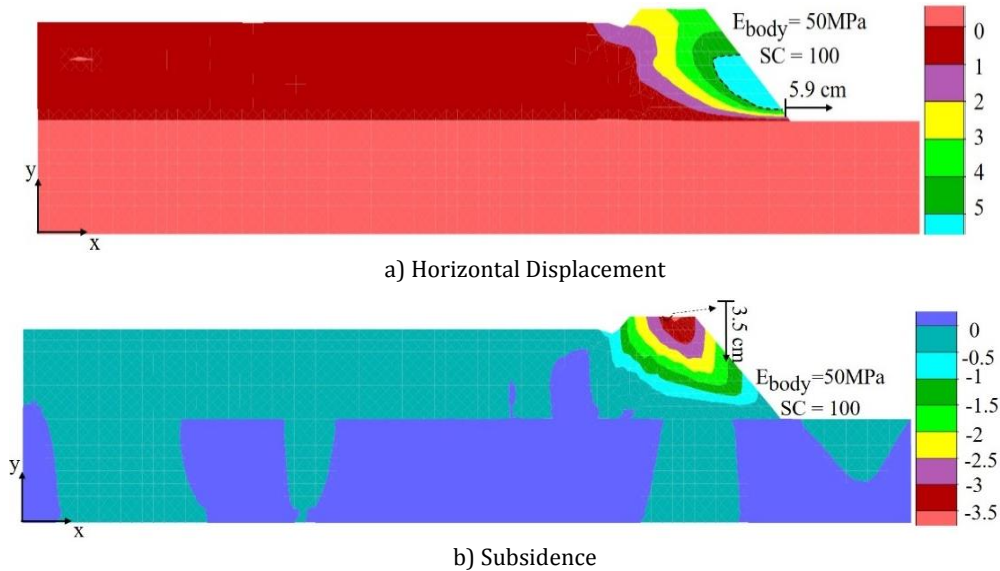


Fig. 2. Contours of maximum displacement occurring from the changes in the stiffness contrast between the foundation and dam body.

The stiffness contrast between the foundation and the tailings can also affect the displacements of the dam body. Figure 6 depicts the horizontal and vertical displacement variation for stiffness contrasts of 500 to 2500 between the foundation and tailings, where the elastic modulus of the tailings varies from 2 to 10 MPa.

value of stiffness contrast and stays contrast afterward. The same trend with a sharper decrease is observed in the subsidence amount where no significant decrease is observed in the maximum displacement after a stiffness contrast of 850. The maximum horizontal displacement and subsidence were observed as 3.56 and 2 cm, respectively, for a stiffness contrast of 500.

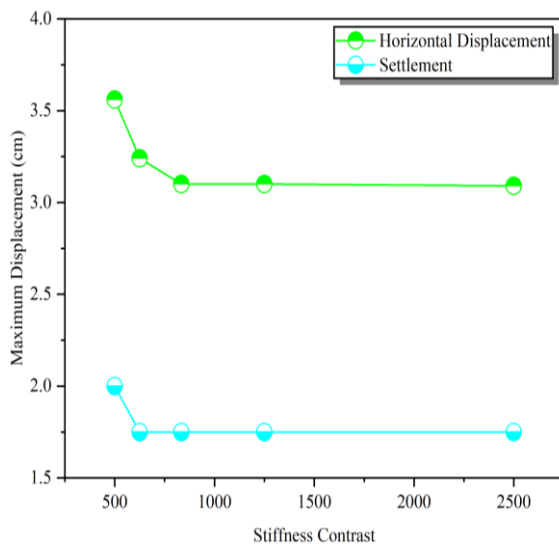


Fig. 6. Displacement variation versus stiffness contrast between dam foundation and tailings.

According to Figure 6, the horizontal displacements decrease with the increasing stiffness difference between the foundation and the tailings. This trend continues to a specific

As the stiffness contrast of the foundation and the tailings increases, the liquefaction coefficient is also affected, which is shown in Figure 7. The figure shows that the liquefaction occurred at low values of the stiffness contrast between the foundation and the tailings, while at high values, liquefaction did not occur. In some cases, as the stiffness contrast of the foundation and the tailings increases, there is no change in the maximum liquefaction coefficient while the extension of the excess pore pressure is shrunk. It should be noted that by increasing the stiffness contrast ratio to 2500 the maximum liquefaction coefficient in tailings has been reduced to 0.5 which may ensure the stability of the tailings in terms of liquefaction. Whereas, at low stiffness contrast ratios, liquefaction in the tailings has inevitably occurred, which can threaten the stability of the dam.

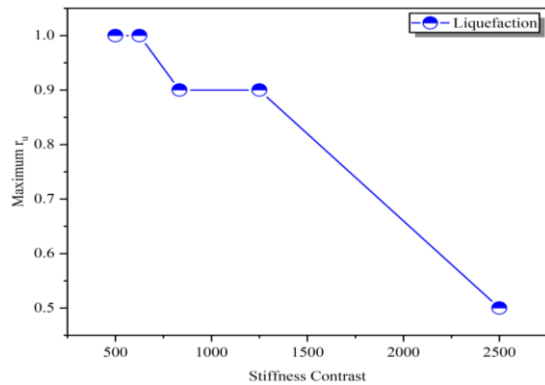


Fig. 7. Liquefaction coefficient in the tailings versus stiffness contrast between foundation and tailings.

In addition to the elastic modulus, the effect of Poisson's ratio variation is investigated on the horizontal displacements, subsidence, and liquefaction. The considered variation ranges of the Poisson's ratio are shown in Table 3.

Table 3. Variation of Poisson's ratio

Parameter	ν	K(MPa)	G(MPa)
Body Dam	0.25-0.4	13.3-33.33	7.14-8
Tailings	0.25-0.4	3.33-8.33	1.79-2

The results of the maximum changes in horizontal displacement and subsidence caused by changes in the Poisson's ratio of the dam body can be seen in Figure 8. According to this figure, the horizontal displacement and subsidence increase significantly with the Poisson's ratio growth.

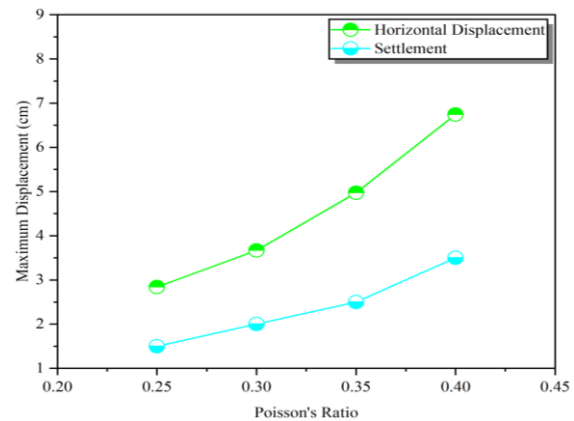


Fig. 8. Displacement occurring from the changes in Poisson's ratio of body dam.

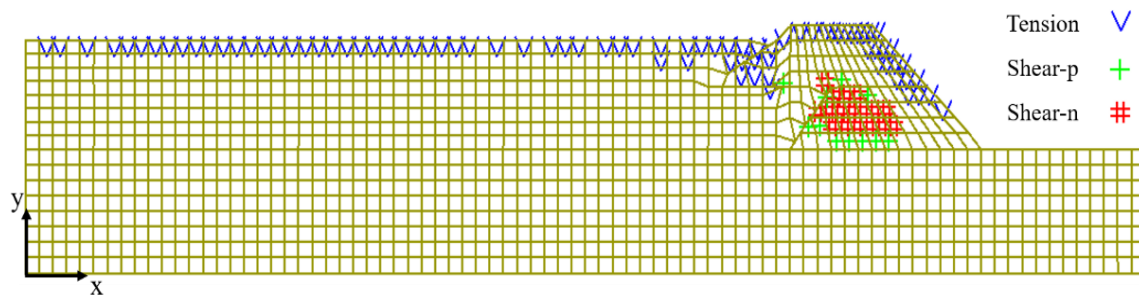


Fig. 9. Plastic zones at $\nu_{body\ dam} = 0.4$

According to Figure 8, the lowest horizontal displacement occurred for Poisson's ratio equal to 0.25 and its value is 2.84 cm. Moreover, the maximum horizontal displacement occurred at 6.74 cm and 0.4 for Poisson's ratio occurred. In other words, with a 60% increase in the Poisson's ratio, the maximum horizontal displacement of the dam body has increased by approximately 140%. The subsidence in the body of the dam has increased by 135% with a 60% increase in the Poisson's ratio, therefore, for a Poisson's ratio of 0.4, the maximum subsidence has reached 3.5 cm. With increasing the Poisson's ratio of the dam body, the displacements have increased, which is due to the higher lateral deformability in the higher Poisson's ratio. Therefore, by applying the wave in the two directions, the displacement is increased in both horizontal and vertical directions .

In general, the maximum size of horizontal displacements and subsidence is significant and in

the range of 1.5-7 cm. However, it is notable to find out whether these movements are temporary or permanent. According to Figure 9, it can be seen that the displacements have entered the plastic stage and parts of the dam body have yielded under shear and tensile stresses.

The outer part of the dam body is mostly under tensile stress and the inner part is under shear stress. Therefore, despite the relatively small amount of horizontal and vertical displacements, regions of the dam have reached the plastic stage and the displacements are irreversible. This phenomenon may threaten the dam structure over time.

The Poisson's ratio of waste materials may change during the construction of the dam and the life of the dam; Therefore, the effect of these changes on displacements and liquefaction due to seismic load is discussed. It was observed that with increasing the Poisson's ratio of the dam

body, the horizontal displacements and subsidence of the dam body as well as the liquefaction coefficient increase. It is expected to observe a similar trend with increasing Poisson's ratio of tailings. Considering Poisson's ratio of the tailings in the range of 0.25 to 0.4 and applying the sinusoidal seismic loads, variations in horizontal displacements and subsidence were examined. The results are illustrated in Figure 10.

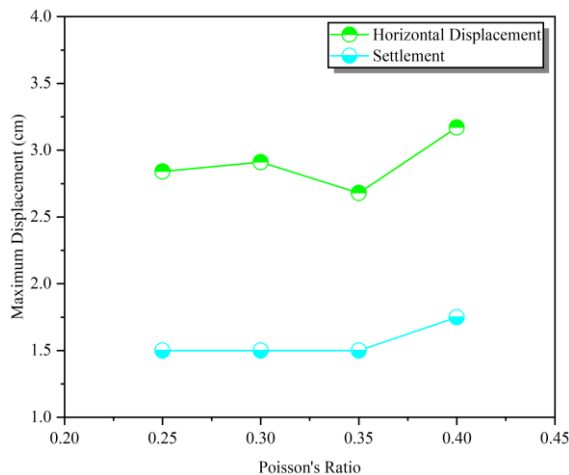


Fig. 10. Observed displacements occurred from variation in the Poisson's ratio of tailings.

According to figure 10, the maximum horizontal displacement has generally increased with increasing Poisson's ratio of tailings. Also, the subsidence values have increased with increasing the Poisson's ratio of tailings, by 1.6 times and the maximum subsidence has increased almost 1.2 times, from 1.5 to 1.75 cm. Thus, in general, changes in Poisson's ratio of tailings do not cause a significant change in horizontal displacements and subsidence.

The maximum liquefaction coefficient is another criterion that has been considered to investigate the changes in Poisson's ratio in this study. By increasing the Poisson's ratio of tailings, liquefaction in this range is monitored at each stage. The results show, that increasing the Poisson's ratio does not vary the maximum coefficient of liquefaction in the tailings. However, it can be seen in detail that these changes affect the maximum liquefaction coefficient in the dam body. The results of these two analyses are presented in Figure 11.

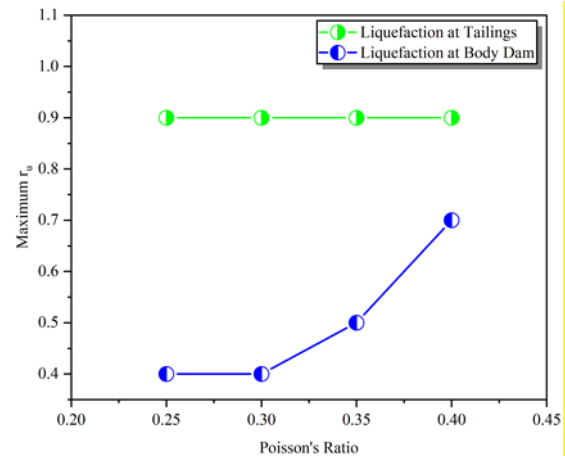


Fig. 11. Liquefaction coefficient variation against Poisson's ratio in tailings.

This figure depicts that increasing the Poisson's ratio of tailings has increased the maximum liquefaction coefficient in the dam body. The maximum liquefaction coefficient in the dam body for Poisson's ratio of 0.25 is equal to 0.4. Also, with increasing this ratio, the maximum liquefaction coefficient has gradually increased until it has reached its maximum value of 0.7. Although a liquefaction coefficient of 0.7 is not considered critical according to most researchers, some studies have considered this amount to be critical. In other words, this amount can put materials on the verge of liquefaction. Figure 12 shows the liquefaction contours for different values for Poisson's ratio of tailings.

It is observed that the maximum liquefaction coefficient of the tailings did not change with an increasing Poisson's ratio. However, the maximum liquefaction coefficient in the dam body has gradually increased and the liquefaction has been extended to the toe of the dam slope. It is noteworthy that the maximum liquefaction coefficient of the dam body did not change with increasing Poisson's ratio from 0.25 to 0.3, while the area with the maximum liquefaction coefficient in the dam body has expanded. Also, in all four levels of the Poisson's ratio from 0.25 to 0.4, the tailings are liquefied and their maximum liquefaction coefficient is 0.9 which exceeds the critical limit of 0.8.

Moreover, to better understand the effect of the two parameters of stiffness contrast and Poisson's ratio on liquefaction, the combined effect of these two parameters has been examined and the results are shown in Figure 13.

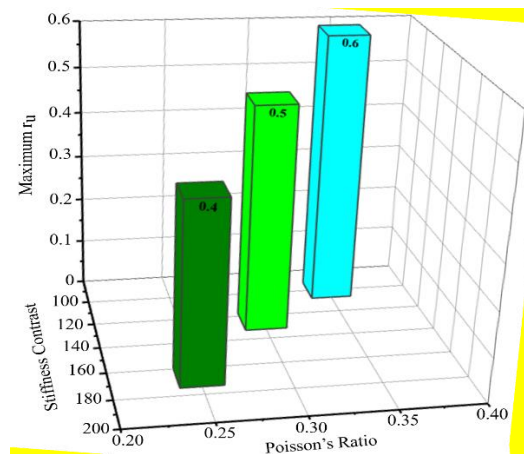


Fig. 13. The effect of Stiffness contrast and Poisson's ratio on liquefaction factor at body dam.

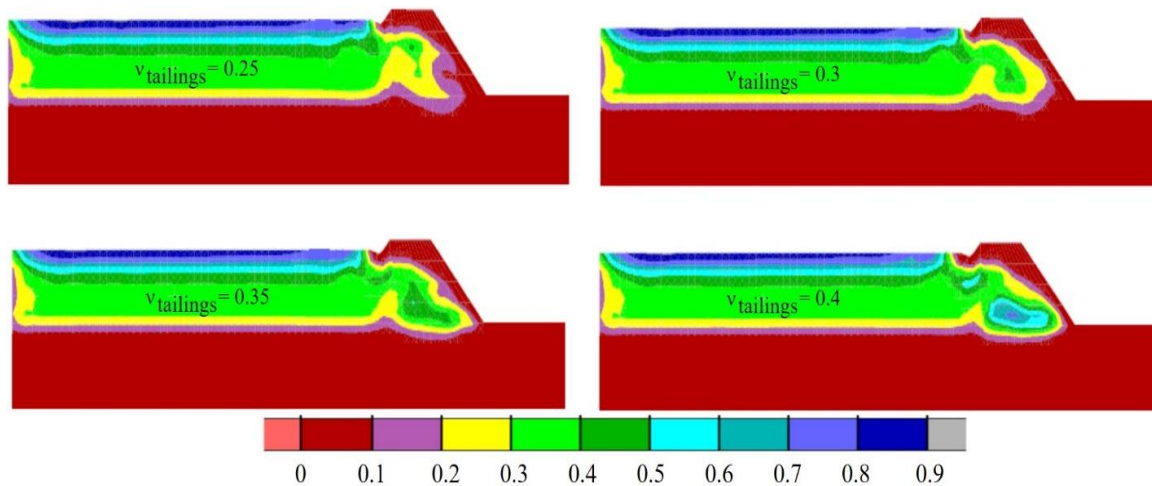


Fig. 12. Contours of liquefaction occurring from the changes in the Poisson's ratio of tailings.

According to figure 13, by increasing Poisson's ratio and decreasing the stiffness contrast between the foundation and the dam body, the liquefaction coefficient has increased; However, the liquefaction occurrence conditions are not provided. It should be noted that by increasing the Poisson's ratio, the dam body would be more susceptible to deformation. On the other hand, by reducing the stiffness contrast the wave propagates with the less damping inside the dam body due to the increase in the elastic modulus of the dam body. This phenomenon is observed in the coefficient of liquefaction.

5. CONCLUSION

The difference in material stiffness can cause changes in the seismic response of tailing dams such as displacement and liquefaction. First, the elastic modulus of the dam body and the tailings were changed in a reasonable range, and after applying a sinusoidal seismic load for one second, displacement and liquefaction parameters were

monitored and investigated for each set of parameters. The effect of Poisson's ratio variation is then mentioned and the results were analyzed. The following results have been obtained from the present study:

- By increasing the elastic modulus of the dam body, the maximum horizontal displacement and the subsidence grew 2.3 and 3.5 times, respectively, and the maximum liquefaction coefficient in the dam body is doubled.
- The most sensitive parameter against stiffness contrast reduction between tailings and dam body is subsidence.
- The liquefaction coefficient decreases as the stiffness contrast between the dam foundation and tailings increases. The stiffness contrast values from 2500 to 500, the maximum horizontal displacement and maximum subsidence

would increase 1.15 times, and the maximum liquefaction coefficient is doubled in the tailings.

- Increasing the dam body Poisson's ratio in the reasonable range of 0.24 to 0.4, the maximum horizontal displacement, subsidence, and liquefaction coefficient rise 2.4, 2.3, and 1.75 times, respectively.
 - Growing the Poisson's ratio of tailings, the maximum liquefaction coefficient of the tailings did not change; however, this increase has increased the maximum liquefaction coefficient of the dam body. By increasing the Poisson's ratio of tailings by 1.6 times, the maximum horizontal displacement, subsidence, and liquefaction coefficients grow 1.1, 1.2, and 1.75 times, respectively.

To sum up, the difference in material stiffness and Poisson's ratio of the dam material has a positive effect on the displacement and liquefaction of the dam body and tailings, subjected to seismic load. Therefore, due to the gradual variation of the tailing's geomechanical properties during its life, the mechanical properties of the dam material should be continuously monitored to predict or if possible, prevent them from failure and crossing the critical liquefaction limit.

REFERENCES

- [1] K.Pitilakis, "Site effects," In Recent advances in earthquake geotechnical engineering and microzonation, Springer, Dordrecht,(2004) pp. 139-197.
- [2] Pitilakis, K., O. J. Ktenidou, P. Apostolidis, D. Raptakis, M. Manakou, K. Makropoulos, and D. Diagourtas. "Experimental and theoretical studies of topographic effects," Proc. 16th ICSMGE (2005), pp. 175-182.
- [3] D. Assimaki, E. Kausel, and G. Gazetas, "Soil-dependent topographic effects: a case study from the 1999 Athens earthquake," Earthquake Spectra 21, no. 4 (2005), pp. 929-966.
- [4] G. D. Bouckovalas and A. G. Papadimitriou, "Numerical evaluation of slope topography effects on seismic ground motion," Soil Dynamics and Earthquake Engineering 25, no. 7-10 (2005), pp. 547-558.
- [5] H. Havenith, D. Jongmans, E. Faccioli, K. Abdrakhmatov, and P. Bard, "Site effect analysis around the seismically induced Ananevo rockslide, Kyrgyzstan," Bulletin of the Seismological Society of America 92, no. 8 (2002), pp. 3190-3209.
- [6] S. Wang and H. Hao, "Effects of random variations of soil properties on site amplification of seismic ground motions," Soil Dynamics and Earthquake Engineering 22, no. 7 (2002), pp. 551-564.
- [7] H. B Havenith, M.Vanini, D.Jongmans, & E. Faccioli, "Initiation of earthquake-induced slope failure: influence of topographical and other site specific amplification effects," Journal of seismology 7, no. 3 (2003), pp. 397-412.
- [8] P. N. Ā. Psarropoulos, Y. Tsompanakis, and Y. Karabatsos, "Effects of local site conditions on the seismic response of municipal solid waste landfills," Soil Dynamics and Earthquake Engineering 27, no. 6 (2007), pp. 553-563.
- [9] C. Bourdeau and H. B. Havenith, "Site effects modelling applied to the slope affected by the Suisamy earthquake (Kyrgyzstan, 1992)," Engineering Geology 97, no. 3-4 (2008), pp. 126-145.
- [10] Y. Mitani, F. Wang, A.C. Okeke and W. Qi, "Dynamic analysis of earthquake amplification effect of slopes in different topographic and geological conditions by using ABAQUS," In Progress of Geo-Disaster Mitigation Technology in Asia, Springer, Berlin, Heidelberg, (2013), pp. 469-490.
- [11] J. R. Moore, V. Gischig, F. Amann, M. Hunziker, and J. Burjanek, "Earthquake-triggered rock slope failures: Damage and site effects," In Proceedings 11th International & 2nd North American Symposium on Landslides, vol. 1, Banff, Canada: CRC Press, (2012), pp. 869-875.
- [12] F. Gouveia, R. C. Gomes, I. F. Lopes, and A. B. Author, "Influence of stiffness contrast in non-horizontally layered ground on site effects," In Proc. of the 15th world conference on earthquake engineering. 2012.
- [13] A. Azhari and U. Ozbay, "Role of geometry and stiffness contrast on stability of open pit mines struck by earthquakes," Geotechnical and Geological Engineering 36, no. 2 (2018), pp. 1249-1266.
- [14] D. Solans, E. Skiada, S. Kontoe, and D. M. Potts, "Canyon topography effects on ground motion: Assessment of different soil stiffness profiles," Obras y Proyectos, no. 25 (2019), pp. 51-58

- [15] A. Azhari, H. S. Isfahani, and K. E. Heydari, "Effect of geometry and material of municipal solid waste landfills on seismic response," In Proceedings of the Institution of Civil Engineers-Waste and Resource Management, Thomas Telford Ltd, (2021), pp. 1-16.
- [16] M. Najafi and A. Yarahmadi Bafghi, "Analysis of sustainability and environmental management of tailings dam (Case study: tailings dam Esfordi Phosphate Mine Processing Factory)," 5th Iranian Conference on Engineering Geology and Environment, Tehran, 2007 (In Persian).
- [17] J. Luis, G. Diez, J. G. Galindo, and A. Soriano, "Adjustment of a numerical model for pore pressure generation during an earthquake," Plos one 14, no. 9 (2019), e0222834.
- [18] M. P. Byrne, "A cyclic shear-volume coupling and pore pressure model for sand," Second Int. Conf. Recent Adv. Geotech. Eng. soil Dynamic, (1991), pp. 47-55.
- [19] Itasca Consulting Group, Inc, FLAC version 7.0: Fast Lagrangian analysis of continua. User's guide. ICG, Minneapolis, 2011.
- [20] O.Vargas, R.Ortiz, and F. Flores, "Liquefaction Analysis Using Pore Pressure Generation Models During Earthquakes," In From Fundamentals to Applications in Geotechnics, IOS Press, (2015), pp. 1057-1064.
- [21] A.Asaadi, M. Sharifipour, & K. Ghorbani, "Numerical simulation of piles subjected to lateral spreading and comparison with shaking table results," Civil engineering infrastructures journal 50, no. 2 (2017), pp. 277-292.
- [22] "Earthquake Design Regulations (Standard 2800)," Fourth Edition, Building and Housing Research Center, Ministry of Housing and Urban Development of Iran, no. Standard 2800, 2014.